Discrimination Based Banding Assessment

Yousun Bang, Zygmunt Pizlo, and Jan P. Allebach
Purdue University
West Lafayette, IN/USA

Norman Burningham
HP Company
Boise, ID/USA

Abstract

Printer banding is an important quality issue; and it has been analyzed and assessed by many researchers. However, little literature has focused on the study of the relationship between physically measured banding and perceived banding. In this paper we propose an experimental methodology for assessing banding which is based on the observer's ability to discriminate between images with different levels of banding. We describe our banding measurement technique, and analyze the banding of three monochrome laser printers. We also conduct psychophysical experiments using the method of constant stimuli. Our results show that the Weber fraction for discriminating banding is statistically constant over the printers despite differences in the spectral content of the banding associated with each printer. This suggests that banding discrimination is similar to many other perceptual phenomena (Weber's law holds).

Introduction

Banding is a printer artifact that is due to the fluctuations of the internal printer components. It usually appears as nonuniform light and dark lines across a printed page perpendicular to the direction in which the paper passes through the printer. Banding is one of the most serious print quality problems in the electrophotographic printing industry.

For laser printers, it is known that the velocity variation of the optical photo-conductor drum is a main cause of banding,[1, 2] and much research has been done to reduce it.[3, 4, 5] Researchers have also tried to quantify the amount of banding in a printed page.[6, 7] Banding is usually considered as a one dimensional quasi-periodic signal; and it is often modeled as a sinusoidal, or square wave signal.[8] Since banding is judged by human observers, it is not only a physical phenomenon but also a perceptual phenomenon. Much work has been done to subjectively evaluate image quality; and studies on the perceptibility of banding have been reported in some papers.[8, 9, 10, 11]

Those efforts have significantly contributed to our understanding of banding; but little research has focused on finding the relationship between physically measured banding and perceived banding. A method for physically measuring banding may provide an absolute metric for a given printer; but that metric may not have perceptual meaning. On the other hand, the subjective evaluation of banding considers human perceptual factors; but it may not give an absolute measure for a given printer.

The goal of this research is to establish a perceptual scale of banding which is based on psychophysics, but which also gives an absolute measure associated with a given printer. Our approach to this problem is shown in Fig. 1. The key idea is to measure the observer's ability to discriminate between two prints with the same content, but which have different levels of banding. One of the prints has only the banding that is intrinsic to the printer, and serves as the reference stimulus. The other print contains this intrinsic banding plus a small amount of added extrinsic banding, and serves as the test stimulus. As the level of intrinsic banding increases, a larger amount of extrinsic banding will be required for the observer to be able to reliably determine which of the two prints contains the added banding. Thus, we can indirectly measure the level of intrinsic banding for a single printer.

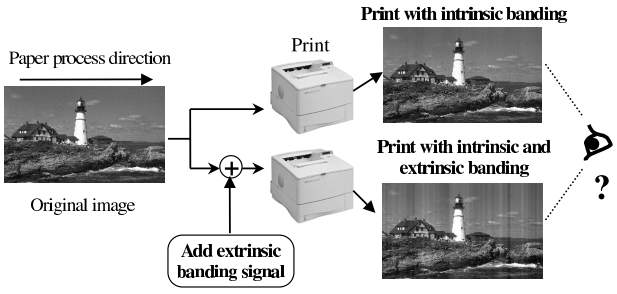

Figure 1: *Overview of our approach to the study of banding discrimination.*

Although this approach to banding assessment is in principle straightforward, in practice, properly generating the print with extrinsic banding is a very complex process. This is because the extrinsic banding must closely mimic the intrinsic banding, or else the observer's ability to discriminate between the reference and test prints will not be a reliable indicator of the relative levels of banding in these two prints.

Success in this endeavor depends on a number of considerations.

First, we must properly extract a prototype banding signal that can be used as the source of extrinsic banding. Second, we must work in the output space of the printer. This requires a transformation to this space from the input space of the printer, and back again after the extrinsic banding signal has been added. To do this correctly, all components of the imaging pipeline must be properly calibrated. Third, the strength of the intrinsic banding is tone-dependent. Fourth, we must avoid saturating the range of the printer when we add the banding signal. Fifth and finally, the electrophotographic process as realized in low cost desktop printers is highly unstable. There is a great deal of variability from print-to-print and even within a single print. This makes accurate estimation of all the aforementioned quantities, that are necessary to generate the print with extrinsic banding, an extremely challenging task.

The remainder of the paper is organized as follows. In the next section, we discuss how we measure and analyze banding. Then we describe how we generate images with extrinsic banding and our experimental procedure. Finally, we present the results of our experiments and discuss the ramifications of those results.

Measurement and Analysis of Banding

In this section, we describe our banding measurement technique and introduce Gabor banding power as a banding metric. We also report the measurement of the gray level dependent banding efficiency function.

In this paper we analyze the banding for three laser printers: *Printer A, Printer B*, and *Printer C*. For our banding measurement we also use a flatbed scanner[1]. To calibrate all these devices, we design a test page with uniform patches having 20 levels of gray value with nominal absorptance 0.05, 0.10, 0.15, ..., 0.95, and 1.00. For each printer we obtain a calibration curve by printing the test page at 600 dpi (dots/in) and measuring the luminance Y values with a Gretag SPM 50 spectrophotometer[2]. We calibrate the scanner in a similar manner.

Gabor Banding Power

The procedure for obtaining the one dimensional banding signal is as follows[12]: First, we design a 7 in $\times$ 0.5 in uniform test patch with absorptance 0.5 and create it as a TIFF image. To control the halftone features of each printer, we use software which generates periodic clustered dot halftones using the pulse width modulation capability of the printer. We print the test patch at 600 dpi, and we then scan it at 600 dpi using the flatbed scanner. We convert the scanned digital values to absorptance by applying the scanner calibration curve.

[1]Heidelberg Saphir Ultra2: Heidelberg USA, Inc., Kennesaw, GA 30144

[2]Gretag SPM 50: Gretag Aktiengesellschaft, Zürich, Switzerland

We average the absorptance values in the direction perpendicular to the printer process direction to get a one dimensional banding profile. We subtract the mean value of this signal, and then compute the N-point Fast Fourier Transform, where N is the length of the 1-D banding signal. The one dimensional banding profile and its spectrum for Printer A are shown in Figs. 2 (a) and (b).

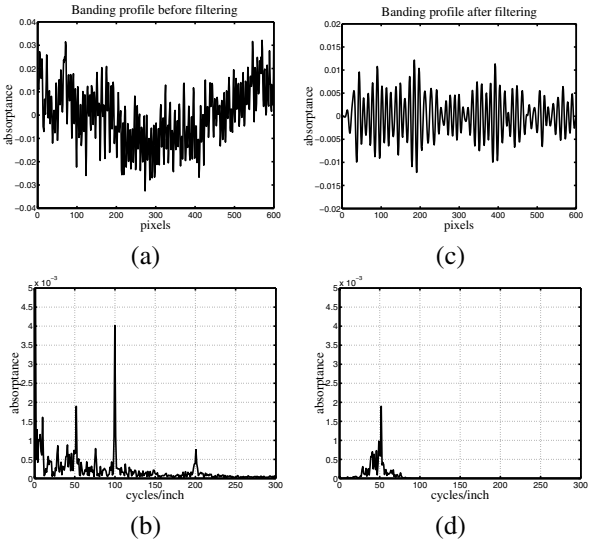

Figure 2: (a) Banding profile and (b) its spectrum before Gabor filtering and (c) banding profile and (d) its spectrum after Gabor filtering for Printer A.

For Printer A and Printer C, the principal banding frequencies are observed around 50 cycles/in; and for Printer B the principal banding frequency is around 18 cycles/in.

The two dimensional Gabor function has been used to model the spatial summation properties of the receptive fields of simple cells in the visual cortex.[13, 14, 15] Incorporating this model in our banding analysis, we use a one dimensional Gabor function

$$g(x) = \exp(-\frac{x^2}{2\sigma^2})\cos(2\pi u_0 x), \qquad (1)$$

to design a band-pass filter whose center frequency is the principal banding frequency. Here σ is the standard deviation of the Gaussian factor which determines the size of the receptive field, and u_0 is the spatial frequency of the cosine factor. Thus σ and u_0 determine the spatial frequency bandwidth of the simple cells. Neurophysiological researchers have reported that the half-response spatial frequency bandwidth of simple cells is in the range of 0.4 to 2.6 octaves.[16] To design a Gabor band-pass filter, we choose a 1.0 octave bandwidth, and let u_0 be the principal banding frequency (50 cycles/in for Printer A and Printer C and 18 cycles/in for Printer B). With this Gabor filter, we process the banding profile obtained above. Figures 2 (c) and (d) show the plots of the one dimensional banding profile and its spectrum after Gabor band-pass filtering.

We now estimate the power spectral density of the Gabor band-pass filtered signal using a periodogram method.

The periodogram of a signal $x[n]$ is given by the following formula:

$$P_{xx}[k] = \frac{1}{N}|X[k]|^2 \text{ for } k = 0, 1, ..., N-1, \quad (2)$$

where $X[k]$ is the Fast Fourier Transform of $x[n]$, and N is the length of $x[n]$.

Let us denote by $x[n]$ the one-dimensional Gabor band-pass filtered banding signal. We calculate the banding average power P of $x[n]$ from the estimated power spectral density:

$$P = \frac{1}{N}\sum_{k=0}^{N-1} P_{xx}[k] = \frac{1}{N^2}\sum_{k=0}^{N-1}|X[k]|^2, \quad (3)$$

$$= \frac{1}{N}\sum_{n=0}^{N-1}|x[n]|^2. \quad (4)$$

The last equality holds by Parseval's Theorem. By taking the square root of the banding average power, we obtain the banding root mean square power (RMS power):

$$P_{rms} = \sqrt{P} = \sqrt{\frac{1}{N}\sum_{n=0}^{N-1}|x[n]|^2}. \quad (5)$$

Here, we can see that the banding RMS power P_{rms} of $x[n]$ is equal to the (biased) standard deviation of $x[n]$ since $x[n]$ has zero mean. In this paper, we define the banding average power P and the RMS power P_{rms} as *Gabor banding power* and *Gabor banding RMS power*, respectively; and we will use these quantities for our banding metric.

We have measured the Gabor banding RMS power for the three printers and the results are shown in Table 1. The table indicates that Printer B has 1.3 times more banding RMS power than Printer A, and Printer C has 1.4 times more than Printer A.

Table 1: **Gabor banding RMS power.**

Printer	Principal Banding Frequency (cycles/in)	Gabor Banding RMS Power (in absorptance)
Printer A	50	0.0034
Printer B	18	0.0044
Printer C	50	0.0049

Banding Efficiency Function

Since the strength of the banding signal depends on gray level, we measure the banding power at different gray levels and obtain a gray level dependent measure of banding for each printer. In this paper we will call this function the *banding efficiency function* (BEF).

We designed a test page consisting of twenty 7.0 in $\times$ 0.35 in uniform test patches with absorptance values uniformly spaced between 0 and 1. There will be some variation of the measurement from print to print and also within each print, so we repeated the measurement for 21 different pages, each of which has the 20 test patches randomly ordered. We computed the banding power for each test patch in the units of absorptance squared as previously described. However, instead of using a Gabor band-pass filter, we applied an ideal narrow band-pass filter around the principal banding frequency to make the computed banding power more closely reflect the spectral magnitude at the principal banding frequency. The cutoff frequencies of these filters were 45 and 55 cycles/in for both Printer A and Printer C, and 15 and 25 cycles/in for Printer B. Figures 3 (a), (b), and (c) show the banding efficiency functions measured for Printer A, Printer B, and Printer C. The figures show the average banding powers with 95% confidence intervals as well as polynomials fitted to this data.

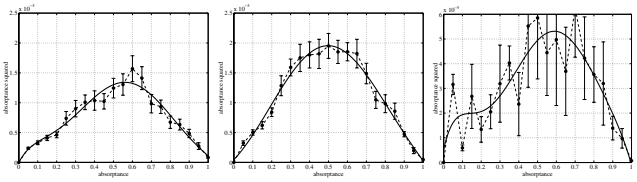

(a) (b) (c)

Figure 3: *The banding efficiency functions measured from (a) Printer A, (b) Printer B, and (c) Printer C.*

All three banding efficiency functions have very similar shapes; and their peak values occur around the mid-tone gray level. To obtain a normalized banding efficiency function in units of absorptance, we take the square root of the banding power, fit a 6th order polynomial function, and then divide all the values by the peak value. Henceforth, we will denote this normalized BEF by $\eta(a)$, where a is the absorptance.

Banding Discrimination Experiments

In this section, we report our psychophysical experiments and the results.

Preparation of Image Samples

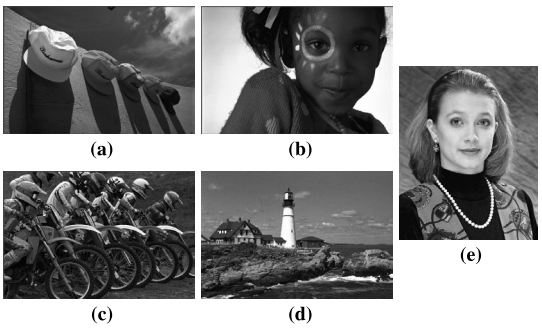

Figure 4: *Five original images that were chosen for our experiments: (a) Cap, (b) Kid, (c) Race, (d) Lighthouse, and (e)Portrait.*

We carefully selected five original image contents for our experiments: *Cap, Kid, Race, Lighthouse, and Portrait*

sho-wn in Fig. 4. The five original images were preprocessed to have appropriate size and desirable contrast levels for comfortable viewing. We mounted all the prints inside hinged neutral gray mats[3] consisting of a cover frame with a rectangular opening on top of a mat board backing.

Prototype Banding Signal

To generate the prints with extrinsic banding, we use a prototype banding signal. In the previous section, we discussed the procedure for extracting a one-dimensional banding signal for each printer. For our prototype banding signal, we used constant patches with absorptance 0.5, since as shown in Fig. 3, this is near the peak in the BEF for each printer. We filtered this 1-D banding signal in the spatial domain using a 5th order *Butterworth* band-pass filter with the cutoff frequencies, 5 cycles/in and 80 cycles/in for each printer. We use a relatively broad band filter here to preserve the physical characteristics of the banding signal while removing the very low frequencies that are the cause of streaks and other gross variations in tone that are not associated with banding. We expanded the obtained banding signal into two dimensions by back-projection.

Throughout the paper we will call this two dimensional banding signal the *prototype banding signal* and will denote it by $b[m, n]$ (in absorptance), where m and n are the pixel indices. By repeating the above procedure for the three printers Printer A, Printer B, and Printer C, we obtained three different prototype banding signals.

Image with Extrinsic Banding

For each original image $o[m, n]$, we generate an image with extrinsic banding represented by $e[m, n]$ in digital gray values, so that when this digital image with the extrinsic banding is sent to a printer, the hardcopy print will have both intrinsic and extrinsic banding. Figure 5 shows the procedure for generating a digital image with extrinsic banding. We apply the printer calibration curve to the original input image $o[m, n]$ to get $x[m, n]$ in the printer space (Gretag luminance Y space), and convert $x[m, n]$ to units of absorptance between 0 and 1.

Since we want to generate several levels of extrinsic banding for our experiments, we use a scaling factor α to control the level of extrinsic banding. When α is 0, we produce an output image which is the exactly same as the original input image (no extra banding is added). When α is 1, the amount of extrinsic banding is equivalent to that of the intrinsic banding in the output image. In other words, α is the amount of extrinsic banding relative to the amount of intrinsic banding.

We next compute the banding gain which prevents clipping of the image with extrinsic banding added, in highlights and shadows, when α is large. The banding gain

$$\rho[m,n] = \begin{cases} \alpha\eta(x[m,n]), \text{ if } \alpha\eta(x[m,n])b_{max} < r[m,n], \\ \dfrac{r[m,n]}{b_{max}}, \qquad \text{otherwise}, \end{cases} \tag{6}$$

[3]MatShop/Island Art Shop: Bellingham, WA 98226

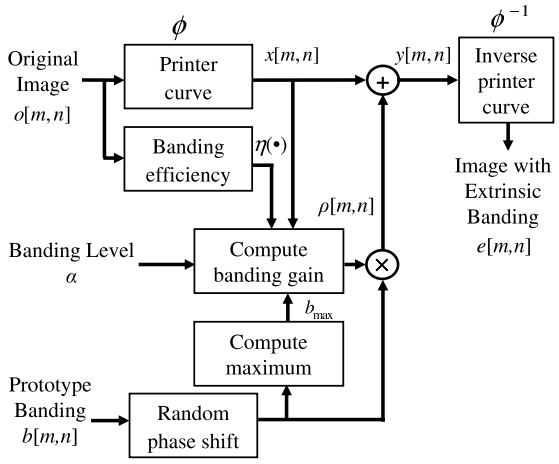

Figure 5: *Procedure for generating digital image with extrinsic banding.*

where $r[m, n] = min\{1 - x[m, n], x[m, n]\}$ and

$$b_{max} = max\{|b[m, n]|\}.$$

is computed by multiplying the banding level α by the banding efficiency $\eta(x[m, n])$ when this product is small enough so that clipping will not occur. Otherwise, the gain is set to a value that just scales the extrinsic banding signal to fill the available signal range without clipping.

We then compute the image

$$y[m, n] = x[m, n] + \rho[m, n]b[m, n - n_0], \tag{7}$$

in the printer output space with level α of extrinsic banding by adding the randomly shifted prototype banding $b[m, n - n_0]$ to the input image $x[m, n]$ after multiplication by the banding gain. The random shift n_0 in the process direction accounts for the random phasing of the banding signal from page to page. By applying the inverse printer calibration curve, we obtain the digital image $e[m, n]$ with extrinsic banding.

For each image content, we generated images with eight levels of extrinsic banding 0.0, 0.1, 0.2, 0.3, 0.4, 0.5, 0.6, and 0.7. We selected this range of α so that almost all naive subjects could easily tell the difference between the original images and the images at the 0.7-level of extrinsic banding, whereas about half of the subjects could tell the difference at the middle range where $\alpha = 0.3$.

Method of Constant Stimuli

The method of constant stimuli[17] is one of the classical methods in psychophysics. In this method, reference and test stimuli are presented to the subject on each trial. The level of the test stimulus varies randomly from trial to trial.

We used the method of constant stimuli to measure the thresholds of banding discrimination for the three printers.

We used the five original prints shown in Fig. 4 as the reference stimuli and 40 print samples (5 image contents $\times$ 8 levels of banding) as the test stimuli for our experiment. A total of 18 Purdue graduate students and 33 industry employees participated for Printer A, 16 Purdue students participated for Printer B, and 7 Purdue students participated for Printer C. Before starting the experiment, each subject was shown three example prints to make sure that he/she understood what banding looks like and the range of banding to be presented. The three example prints comprised one print having the highest level of banding (level 0.7), another having the medium level of the banding (level 0.3), and the remaining one having the lowest level of banding (level 0.0).

On each trial, we showed the subject an original reference print and a test print, both of which had the same content. A total of 40 trials were conducted for each session. The subject responded whether the level of banding in the test print looked the same as or greater than the level in the reference; and the subject's responses were collected by user-interface software developed by the experimenter.

We conducted *Probit Analysis*[18] with the collected psychophysical data and estimated the thresholds. The method fits a normal cumulative distribution function to data using the maximum likelihood method. The Gaussian cumulative distribution is a well-known model for fitting data from psychophysical experiments. Probit Analysis provides estimates $\hat{\mu}$ and $\hat{\sigma}$ of the Gaussian mean and standard deviation respectively for each subject's psychometric function. In addition, it also computes the standard errors (SE) of these estimates, which are the estimated variations of $\hat{\mu}$ and $\hat{\sigma}$.

The thresholds, which are the psychological limits to perception, are often of the greatest interest in psychophysics. The absolute threshold is the lowest amount detectable in the stimulus; and the difference threshold is the lowest detectable difference in stimulus. The Gaussian standard deviation of a psychometric function is usually regarded as a measure of the difference threshold. The difference threshold was described mathematically by Weber (*Weber's law*). Over a wide range of the stimulus, the ratio of the difference threshold to the level L of the original stimulus is a constant W called *Weber's fraction*:

$$\frac{\text{Difference Threshold}}{L} = W. \tag{8}$$

In our calculations, $\hat{\sigma}$ has the same units as does α, the level of extrinsic banding relative to that of intrinsic banding. In Eq. (8), we can consider L as the intrinsic banding. Since the abscissa of our psychometric function is the relative level of extrinsic banding, the value of $\hat{\sigma}$ obtained by Probit Analysis represents the relative difference threshold, i.e. Weber's fraction. We will call this relative difference threshold *DL*. For each printer, we computed the average DL and its standard error for each subject. We also pooled all the subjects' data and estimated the psychometric function for all subjects. The results will be presented in the next section.

Results and Discussion

For each printer we estimated each subject's psychometric function and DL using the method of constant stimuli. Figure 6 (a) shows the psychometric function of a typical subject who participated in the experiment for Printer A. For this subject, the estimated DL was 0.16 (in the relative level of extrinsic banding). For each printer we also pooled all

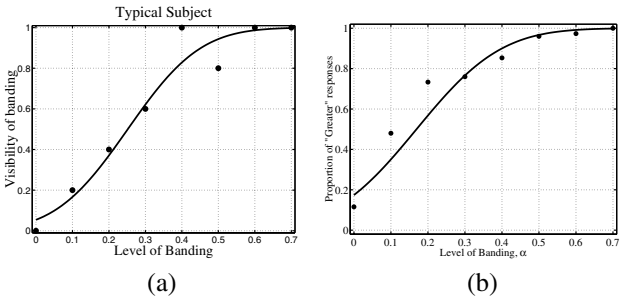

Figure 6: (a) Psychometric function of a typical subject for Printer A. The estimated DL of the subject is 0.16. (b) Psychometric function of 18 pooled Purdue subjects for Printer A.

subjects' data and estimated a psychometric function based on the pooled data. The estimated psychometric function for Printer A based on results pooled from all subjects is shown in Fig. 6 (b). The plot shown on the right looks very similar to the plot on the left, and two plots show that our data were well fitted to a cumulative Gaussian curve.

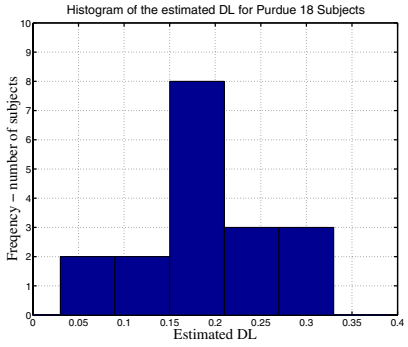

Figure 7: Histogram of the estimated DL's for 18 Purdue subjects in the experiment for Printer A.

We also examined the histograms of the estimated DL's for each printer. Figure 7 presents the histogram for Printer A. The plot shows that the most frequent DL's are located between 0.15 and 0.2.

From each subject's estimated DL, we computed the average DL and its standard error for each printer. The results are shown in Table 2.

Table 2: **Average DL's and standard errors.**

Printer	Average relative DL (Weber's fraction)	Standard Error
Printer A	0.194	0.017
Printer B	0.164	0.012
Printer C	0.160	0.028

The average DL's are about 0.2 for all three printers. This implies that reducing the banding level α by less than 20% would not make a substantial difference in the percept of banding. We conducted a *t*-test for the three DL's in Table 2, and found that with 95% confidence those three numbers are not statistically different. This suggests that the relative DL's are constant over the printers, and Weber's law holds for banding discrimination. This was observed despite the different spectral content of the intrinsic banding associated with the three printers.

Conclusion

In the paper we developed a method of analyzing banding associated with electrophotographic printers, and proposed an experimental methodology for measuring the percept of banding via psychophysical experiments. This methodology is based on the ability of a observer to discriminate between a print containing only banding intrinsic to the printer and a print containing the intrinsic banding plus additional extrinsic banding. We estimated the difference thresholds in banding discrimination for three different printers. We found that Weber's fraction was statistically constant at a value of about 0.2 over the three printers, despite the differences in the spectral content of intrinsic banding associated with each printer. This result suggests that banding discrimination is similar to many other perceptual phenomena (Weber's law holds). The specific value obtained for Weber's fraction indicates the minimum level of improvement required for a reduction in banding to be perceptually significant.

Acknowledgement

We would like to thank the Hewlett Packard Company for supporting this research. We also wish to thank George Kerby for providing the software used to generate the halftones with the three printers.

References

1. D. Hass, "Contrast modulation in halftone images produced by vibration in scanline spacing," J. Imaging Technology, vol. 15, no. 1, pg. 46, (1989).
2. R. Loce, W. Lama, and M. Maltz, "Modeling vibration-induced halftone banding in a xerographic laser printer," J. Elect. Imag., vol. 4, no. 1, pg. 48, (1995).
3. G. Lin, J. Grice, J. Allebach, G. Chiu, W. Bradburn, and J. Weaver, "Banding artifact reduction in electrophotographic printers by using pulse width modulation," J. Imaging. Sci. and Tech, vol. 46, no. 4, pg. 326, (2002).
4. M. Ewe, J. Grice, G. Chiu, and J. Allebach, "Banding reduction in electrophotographic process using piezoelectric actuated laser beam deflection device," Proc. IS&T's NIP16, pg. 276, (2000).
5. C. Chen and G. Chiu, "Banding reduction in electrophotographic process," Proc. IEEE/ASME Int. Conf. Advanced Intelligent Mechatronics, pg. 81, (2001).
6. P. Kane, T. Bouk, P. Burns, and A. Thompson, "Quantification of banding, streaking and grain in flat field images," Proc. IS&T's PICS, pg. 79, (2000).
7. J. Briggs, M. Murphy, and Y. Pan, "Banding characterization for inkjet printing," Proc. IS&T's PICS, pg. 84, (2000).
8. C. Cui, D. Cao, and S. Love, "Measuring visual threshold of inkjet banding," Proc. IS&T's PICS, pg. 84, (2001).
9. D. Rasmussen, E. Dalal, and K. Natale-Hoffman, "Measurement of macro-uniformity: Streaks, bands, mottle and chromatic variations," in Proc. IS&T's PICS, pg. 90, (2001).
10. Y. Ng, "Visual tolerance study with one-dimensional periodic (sinusoidal) and non-periodic (impulse) noise in electrophotographic gray level halftones," Proc. IS&T's 11th International Congress on Advances in Non-Impact Printing Technologies, pg. 493, (1995).
11. W. Wu, E. Dalal, and D. Rasmussen, "Perceptibility of non-sinusoidal bands," Proc. IS&T's NIP18, pg. 462, (2002).
12. W. Jang and J. P. Allebach, "Simulation of Print Quality Defects," Proc. IS&T's NIP18, pg. 543, (2002).
13. J. Daugman, "Uncertainty relations for resolution in space, spatial frequency, and orientation optimized by two-dimensional visual cortical filters," J. Opt. Soc. Amer. A, vol. 2, no. 1, pg. 1160, (1985).
14. N. Petkov and P. Kruizinga, "Computational models of visual neurons specialized in the detection of periodic and aperiodic oriented visual stimuli: bar and grating cells," Biological Cybernetics, vol. 76, no. 2, pg. 83, (1997).
15. A. Kumar and G. Pang, "Defect detection in textured materials using gabor filters," IEEE Trans. Industry Applications, vol. 38, pg. 425, (2002).
16. J.P. Jones and L.A. Palmer, "An evaluation of the two-dimensional gabor filter model of simple receptive fields in cat striate cortex," Neurophysiol., vol. 58, no. 6, pg. 1233, (1987).
17. G. Gescheider, *Psychophysics: Method, Theory, and Application*. Hillsdale, NJ: Lawrence Erlbaum Associates, 2nd ed., 1985.
18. D. Finney, *Probit Analysis*. NY: Cambridge University Press, 3rd ed., 1971.

Biography

Yousun Bang received the B.S. degree in mathematics from Ewha Womans University, Seoul, Korea, in 1994 and the M.S. degree from Purdue University, West Lafayette, IN, in 1999. She is currently pursuing her Ph.D. degree in the School of Electrical and Computer Engineering, Purdue University, West Lafayette, IN. She has been working in Electronic Imaging Systems Laboratory at Purdue University since 2000. Her research interests include electronic imaging systems, image rendering, image quality, and human perception.